Int. J. Solids Structures Vol. 29, No. 3, pp. 345–361, 1992
Printed in Great Britain.

0020–7683/92 $5.00 + .00

A BOUNDARY ELEMENT METHOD FOR PLATE BENDING PROBLEMS

MADHUKAR VABLE and YIKANG ZHANG†
Mechanical Engineering—Engineering Mechanics, Michigan Technological University, Houghton, MI 49931, U.S.A.

(*Received* 14 *August* 1990; *in revised form* 26 *December* 1990)

Abstract—An indirect boundary element formulation is constructed by using a fundamental solution of the biharmonic operator. It is shown that the fundamental solution and its derivatives can be represented by four functions with two integers. The new representation is not only a simpler representation but also reveals a structure that is exploited in the development of an algorithm based on the analytical integration of line and area integrals. The analytical integral values are used to establish continuity requirements on the unknown fictitious densities. Numerical examples consider the consequences of satisfying and violating the continuity requirements by the unknown fictitious densities. It is also shown that if the fictitious density distributions do not satisfy certain conditions then the solution can be affected by the choice of the non-dimensionalizing variables. Numerical examples with a variety of boundary conditions demonstrate the effectiveness and limitations of the proposed algorithm.

1. INTRODUCTION

The various boundary element formulations for plate bending can be broadly categorized as the direct and the indirect formulations. The direct methods are based on the reciprocal theorem. Bezine (1978) and Stern (1979) generated integral equations that related plate displacements, slopes, bending moments and shear forces on the boundary. The indirect formulations are constructed by superposing singular solutions. The unknowns of the problem are fictitious densities but these fictitious densities can be related to jumps in physical variables at the boundary. There are several approaches for constructing the integral equations in indirect methods. Jawson *et al.* (1967) represented the biharmonic equation by two harmonic equations and used the fundamental solution for the harmonic equations to formulate the problem. Altiero and Sikarskie (1978) used Green's function for a circular clamped plate for constructing the integral equations. Both of these indirect formulations produce good numerical results only for certain kinds of boundary conditions. A more general indirect formulation can be constructed by using the fundamental solution of the biharmonic operator, as was done by Tottenham (1979). However, few details about the numerical implementation were discussed. Several investigators (Paris and Leon, 1987; Hartmann, 1986; Abdel-Akher and Hartley, 1989; Vitooraporn and Moshaiov, 1989; Wu and Altiero, 1981) have used the above formulations as the starting point. No study has been conducted that establishes the superiority of one formulation over another.

The fundamental solution of the biharmonic operator is used for constructing the indirect formulation in this work as it is simpler than the direct boundary element method and yet applicable to all types of boundary conditions. The simplicity of the formulation is due to the following two reasons.

(i) A total of eight fundamental solutions are needed in the entire formulation. The direct method uses eight fundamental solutions to relate the boundary data and requires eight more to represent the bending moments (in-plane stresses) and the shear forces (transverse shear stress).

(ii) The highest order of singularity is of order 2 in this work. In the direct formulation the fundamental solutions relating the boundary data also contain a singularity of order 2. However, subsequent differentiation for representing moments and shear forces generates higher order singularities. Evaluation of quantities containing these higher order terms near

† Present address: Walker Engineering and Research Center, Grass Lake, MI 49931, U.S.A.

and on the boundary requires special consideration (see Kaya and Erdogan, 1987; Kutt, 1975; Rudolphi, 1991). It should be emphasized once more that no claim is being made that the indirect method is numerically superior to the direct method. All that is being claimed is that the indirect method is simpler.

The fundamental solutions relating plate displacement to a unit transverse force and a unit bending moment are relatively simple. But to compute slopes, moments and shear forces the fundamental solutions have to be repetitively differentiated. This repetitive differentiation results in long, messy expressions. The problem is further exacerbated if one seeks to evaluate the integrals of these fundamental solutions analytically. In this work an alternative representation is described in Section 3. This representation uses four functions with two integer parameters to describe all the fundamental solutions. This representation, besides being simple, also reveals the structure of the fundamental solutions that can be exploited for the development of the numerical algorithm.

The integral representation of the relevant plate quantities, contains fictitious shear force distribution and fictitious bending moment distribution as the unknowns of the problem. In Section 5 the continuity requirements the fictitious shear force and fictitious bending moment must satisfy are derived and discussed. Situations in which the continuity conditions should be relaxed are also discussed in Section 5. The continuity requirements dictate that the fictitious shear force should be approximated by a Lagrange polynomial and the fictitious bending moment should be approximated by a Hermite polynomial.

In Section 7 the dimensionless variables are defined. It is shown that if certain conditions (analogous to equilibrium) are not satisfied by the fictitious shear force distribution and fictitious bending moment then the results for displacement, slopes and moments can be affected by the choice of non-dimensionalizing variables.

To evaluate the boundary integrals the unknowns were approximated by polynomials over segments of the boundary. Each segment was subdivided into a number of straight line segments. The element over which the unknown is approximated is subdivided to get a better representation of the curvature of the boundary without increasing the number of unknowns. The integrals are evaluated analytically using the general algorithm presented in Vable (1985).

To evaluate the domain integrals the transverse loads were assumed to be constant over small elements of the domain. The shape of these domains can be arbitrary. The domain integrals were converted to line integrals over the boundary of each domain element as described by Zhang (1989). The boundaries of the domain elements are approximated by a set of straight line segments and once more the integrals are evaluated analytically using the algorithm of Vable (1985).

A circular and a square plate subjected to a uniform transverse load with a variety of boundary conditions are used as numerical examples. Results are compared for Lagrange and Hermite polynomial approximations in each example. These results demonstrate the effect of continuity requirements on the accuracy and the matrix conditioning. The results are presented in Section 8.

2. BOUNDARY VALUE PROBLEM

The boundary value problem in terms of a differential equation is presented briefly in order to introduce notation and the sign convection.

Let $w(Q)$ be the small deflection at a point Q on a thin elastic, homogeneous, isotropic plate R. The deflection $w(Q)$ is related to the transverse load $p(Q)$ by the biharmonic operator defined below:

$$Dw_{,ijij}(Q) = p(Q) \quad Q \text{ in } R \quad i, j = x, y \tag{1}$$

where D is the flexural rigidity of the plate. A repeated index implies summation and a comma implies differentiation. The in-plane stresses σ_{ij} are related to the bending moments M_{ij} which can be related to the deflection w as follows:

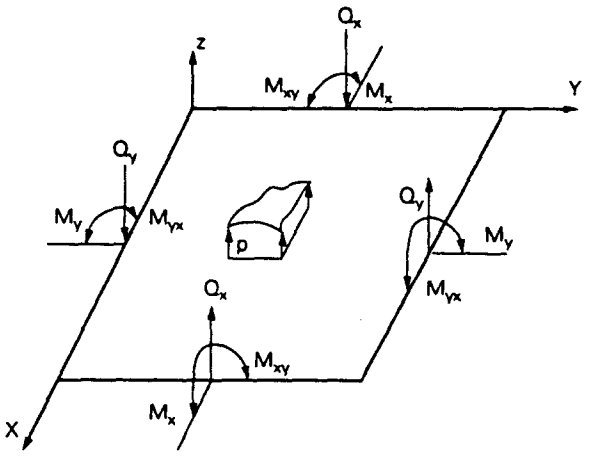

Fig. 1. Positive direction for moments and shear forces.

$$M_{ij} = \int_{-h}^{h} z\sigma_{ij}\,\mathrm{d}z$$

$$= -D[(1-\nu)w_{,ij} + \nu\delta_{ij}w_{,kk}] \tag{2}$$

where $2h$ is the thickness of the plate, ν is Poisson's ratio and δ_{ij} is the Kronecker delta. The shear force Q_i is related to the transverse shear stresses and the deflection w as follows:

$$Q_i = \int_{h}^{h} \sigma_{iz}\,\mathrm{d}z = -Dw_{,jji}. \tag{3}$$

It should be noted (see Fig. 1) that even though $M_{xy} = M_{yx}$ in magnitude, the directions of the moments are different and this difference at a corner results in a corner force (discussed later). At each point on the boundary B except corners, two pieces of information must be specified, as given below:

$$w(Q) = \bar{w} \qquad \text{or} \qquad V_n(Q) = \bar{V} \tag{4a}$$

$$\text{and} \qquad Q \text{ on } B$$

$$w_n(Q) = w_{,i}n_i = \bar{0} \quad \text{or} \quad M_n(Q) = \bar{M} \tag{4b}$$

where the quantities with a bar represent the specified boundary values. n_i represents the direction cosines of the unit normal at point Q on the boundary B. V_n is the equivalent shear force and M_n is the normal bending moment, which can be related to previously defined quantities as follows:

$$M_n = M_{ij}n_in_j = -D(w_{,nn} + \nu w_{,tt}) \tag{5}$$

$$V_n = Q_in_i + \frac{\mathrm{d}}{\mathrm{d}s}(M_{ij}n_it_j)$$

$$= -D(w_{,nnn} + (2-\nu)w_{,ttn}) - D\frac{(1-\nu)}{R}(w_{,tt} - w_{,nn}) \tag{6}$$

where

$$w_{,nn} = w_{,ij} n_i n_j \tag{7a}$$

$$w_{,tt} = w_{,ij} t_i t_j \tag{7b}$$

$$w_{,nnn} = w_{,ijk} n_i n_j n_k \tag{7c}$$

$$w_{,ttn} = w_{,ijk} t_i t_j n_k \tag{7d}$$

and t_i and R represent the direction cosines of the unit tangent and the radius of curvature at point Q respectively on the boundary B.

At each corner the following must be specified:

$$w(Q) = \bar{w}_k \quad \text{or} \quad C_k(Q) = 2M_{nt} = -2D(1-\nu) w_{,ij} n_i t_j = \bar{C}_k \tag{8}$$

where C_k represents the corner force.

The integral representation of eqn (1) is developed by using a fundamental solution, as discussed in the next section.

3. FUNDAMENTAL SOLUTION

Let $G(Q, P)$ represent the displacement at point Q due to a unit transverse force at point P in an infinite plate. Using Fourier transform it can be shown that:

$$G(Q, P) = \frac{1}{8\pi D} r^2 \ln(r) \tag{9}$$

where

$$r^2 = r_i r_i$$

$$r_i = x_i(Q) - x_i(P).$$

Another fundamental solution associated with a unit moment can be generated by considering two transverse forces of equal magnitude but in opposite directions placed along a line, as shown in Fig. 2. The direction of the two forces is chosen to produce a positive deflection to the left of the point P. By superposition the deflection at point Q will be given by:

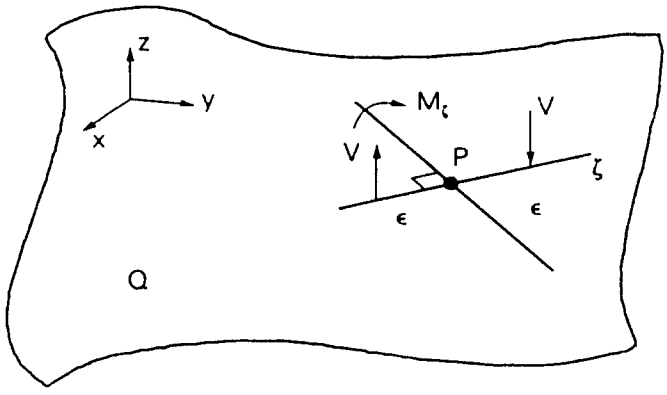

Fig. 2. Positive direction for M_ζ.

$$[G(Q,P-\varepsilon)-G(Q,P+\varepsilon)]V = -\frac{\partial G(Q,P)}{\partial \zeta(P)}(2\varepsilon V) + \text{terms of order } \varepsilon^2.$$

As $\varepsilon \to 0$ let $V \to \infty$ such that $2\varepsilon V \to M_\zeta$. The direction of M_ζ will be perpendicular to the line, as shown in Fig. 2. Thus $-[\partial G(Q,P)]/[\partial \zeta(P)]$ represents the deflection at point Q due to unit moment applied at point P. The superposition principle can once more be invoked to generate integral expressions for the displacement. By distributing a fictitious transverse force V^* and a fictitious moment M_n^*, two line integrals will be generated. The distributed load can be incorporated by distributing the point load over the entire domain R. The following is the integral expression for the deflection w:

$$w(Q) = \oint_B G(Q,P)V^*(P)\,ds(P) + \oint_B \frac{-\partial G(Q,P)}{\partial n(P)} M_n^*(P)\,ds(P) + \iint_R G(Q,P)p(P)\,dx(P)\,dy(P) \quad (10)$$

where s represents the arc length up till point P as measured from some arbitrary point on the boundary B. Fundamental solutions associated with M_{ij}, Q_i, M_n, M_{nt} and V_n can be developed by appropriate differentiation and are presented in detail in Section 3.1. It should be noted that the direction of the line ζ in Fig. 2 is chosen as the normal rather than the tangent direction to the boundary due to numerical consideration only. The numerical discretization discussed in Section 4 results in a system of algebraic equations. The greater the dominance of the diagonal term in the matrix of algebraic equations, the better the numerical accuracy of the solution. When boundary conditions are imposed on the normal moment [eqn (4b)], the singular nature of the fundamental solution yields a singularity contribution (Cauchy's principal value) when point P crosses point Q on the boundary. The singularity contribution is zero if the tangent direction is chosen for the line ζ and is equal to $[M_n^*(Q)/2]$ when the normal direction is chosen for the line ζ. This singularity contribution is added to the diagonal term. Hence the diagonal dominance is increased when the line ζ is in the direction normal to the boundary. Another way of saying the above is that the normal direction for ζ results in strong singular integrals (Fredholm equation of the second kind) while the tangent direction results in weak singular integrals (Fredholm equation of the first kind).

We note that the partial derivative at Q is the negative of the partial derivative at point P. With that in mind we rewrite w and its derivatives as

$$w_{,ijk}(Q) = \oint_B G_{,ijk}(Q,P)V^*(P)\,ds + \oint_B G_{,ijkm}(Q,P)n_m(P)M_n^*(P)\,ds(P) + \iint_R G_{,ijk}(Q,P)p(P)\,dx(p)\,dy(P) \quad (11)$$

where all derivatives are now performed at point Q.

In a similar manner we can write expressions for single and double derivatives at point Q. It is clear from the second integral that we need to perform the differentiation of the fundamental solution four times. These differentiations result in long, messy expressions. The problem is particularly acute if one seeks to integrate these expressions analytically. An alternate notation is presented that is very convenient for presenting not only the various fundamental solutions but also the integrals of the fundamental solutions.

3.1. *Structure of the fundamental solutions*

Most fundamental solutions are linear combinations of four singular functions, as was pointed out by Vable (1985). In plate bending problems there is a more defined structure

to the fundamental solutions, as reported in Zhang (1989). The structure is emphasized by defining the following functions:

$$LG^{[p,q]} = r_x^p r_y^q \ln(r) \tag{12}$$

$$JG^{[p,q]} = \frac{1}{2}\left[\frac{(r_x+\bar{\imath}r_y)^p}{(r_x-\bar{\imath}r_y)^q} + \frac{(r_x-\bar{\imath}r_y)^p}{(r_x+\bar{\imath}r_y)^q}\right] \tag{13a}$$

$$KG^{[p,q]} = \frac{1}{2\bar{\imath}}\left[\frac{(r_x+\bar{\imath}r_y)^p}{(r_x-\bar{\imath}r_y)^q} - \frac{(r_x+\bar{\imath}r_y)^p}{(r_x-\bar{\imath}r_y)^q}\right] \tag{13b}$$

$$PG^{[p,q]} = r_x^p r_y^q \tag{14}$$

where p and q are integers and $\bar{\imath} = \sqrt{-1}$. The complex variables used in eqn (13) are to emphasize the structure of the fundamental solution that will be exploited in the development of the algorithm in Section 4. The algorithm uses only real variables. In Table 1 the fundamental solution and its derivatives are defined in terms of the four functions defined in eqns (12)–(14).

4. PROBLEM DISCRETIZATION

The objective of problem discretization is to generate an algebraic expression. A series of assumptions needs to be made to reduce the line and area integrals to algebraic expressions. These assumptions and their implications are considered next.

4.1. *Line integral*

The general algorithm described in Vable (1985) is used here for the evaluation of line integrals. The algorithm is described briefly here in context of plates. Three assumptions are made.

Assumption 1. Assume the unknown fictitious shear force and the unknown fictitious moment can be represented by a linear combination of M piece-wise continuous functions g_m.

Assumption 2. Assume that each of the m segments can be represented by N_m straight line segments.

Assumption 3. Assume g_m can be expanded about the mid-point by Taylor series.

The three assumptions, in the absence of distributed load ($p = 0$), reduce the line integrals of eqn (11) to:

Table 1. Fundamental solution and its derivatives

$8\pi DG$	$= LG^{[2,0]} + LG^{[0,2]}$
$8\pi DG_{,x}$	$= 2LG^{[1,0]} + JG^{[1,0]} + PG^{[1,0]}$
$8\pi DG_{,y}$	$= 2LG^{[0,1]} + KG^{[1,0]} + PG^{[0,1]}$
$8\pi DG_{,xx}$	$= 2LG^{[0,0]} + JG^{[1,1]} + 2$
$8\pi DG_{,xy}$	$= KG^{[1,1]}$
$8\pi DG_{,yy}$	$= 2LG^{[0,0]} - JG^{[1,1]} + 2$
$8\pi DG_{,xxx}$	$= 3JG^{[0,1]} - JG^{[1,2]}$
$8\pi DG_{,xxy}$	$= KG^{[0,1]} - KG^{[1,2]}$
$8\pi DG_{,xyy}$	$= JG^{[0,1]} + JG^{[1,2]}$
$8\pi DG_{,yyy}$	$= 3KG^{[0,1]} + KG^{[1,2]}$
$8\pi DG_{,xxxx}$	$= 2JG^{[1,3]} - 4JG^{[0,2]}$
$8\pi DG_{,xxxy}$	$= 2KG^{[1,3]} - 2KG^{[0,2]}$
$8\pi DG_{,xxyy}$	$= -2JG^{[1,3]}$
$8\pi DG_{,xyyy}$	$= -2KG^{[1,3]} - 2KG^{[0,2]}$
$8\pi DG_{,yyyy}$	$= 2JG^{[1,3]} + 4JG^{[0,2]}$

$$w_{,ijk}(Q) = \sum_{m=1}^{M} \sum_{p=1}^{N_e} \sum_{q=0}^{NT} \frac{1}{q!} \frac{\mathrm{d}^q g_m}{\mathrm{d}s^q}\bigg|_{s=\bar{s}_p} \times (d_1^{(m)} T_{ijk}^{[q]}(Q, S_p) + d_2^{(m)} T_{ijkn}^{[q]}(Q, S_p) n_n(S_p)) \quad (15)$$

where

$$T_{ijk}^{[q]}(Q, S_p) = \int_{S_p}^{S_{p+1}} (s - \bar{s}_p)^q G_{,ijk}(Q, P)\, \mathrm{d}s(P) \quad (16)$$

and $\bar{s}_p = (S_{p+1} + S_p)/2$ is the mid-point of segment p. NT is the number of terms retained in the Taylor series. For Lagrange linear polynomials, $NT = 1$ and for cubic Hermite polynomials, $NT = 3$. The summations in eqn (15) define the assembly process. By satisfying the boundary conditions at M points a set of algebraic equations in the unknown $d_k^{(m)}$ will be obtained. The integrals in eqn (16) are evaluated using the transformation described next.

4.1.1. *Coordinate transformation.* In Fig. 3 the pth line segment is shown. θ_p is the angle of the line segment measured from the x-axis in the counterclockwise direction. Point A is the intersection of the line segment with the perpendicular line drawn from point Q. The perpendicular distance QA is designated as D_p, while the distance from the mid-point B to point A is designated as C_p. The tangential coordinate t_p is measured from point B. Noting that the influence functions in Table 1 are a linear combination of the functions defined in eqns (12)–(14) the problem reduces to the evaluation of the following four integrals:

$$IL^{[k,i,j]} = \int_{T_p}^{T_{p+1}} t_p^k LG^{[i,j]}\, \mathrm{d}t_p \quad (17)$$

$$IJ^{[k,i,j]} = \int_{T_p}^{T_{p+1}} t_p^k JG^{[i,j]}\, \mathrm{d}t_p \quad (18a)$$

$$IK^{[k,i,j]} = \int_{T_p}^{T_{p+1}} t_p^k KG^{[i,j]}\, \mathrm{d}t_p \quad (18b)$$

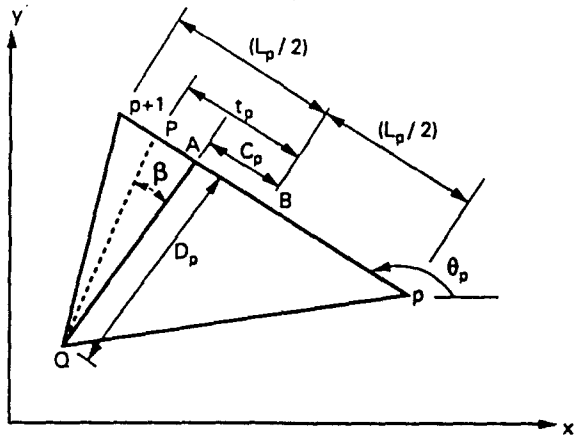

Fig. 3. Geometry of the pth segment.

$$IP^{[k,i,j]} = \int_{T_p}^{T_{p+1}} t_p^k PG^{[i,j]}\,\mathrm{d}t_p \tag{19}$$

where $T_p = -L/2$ and $T_{p+1} = L/2$.

By geometry it can be shown that

$$r_x + \bar{\imath} r_y = -\mathrm{e}^{\bar{\imath}\theta_p}(t_p - B_p) \tag{20}$$

where

$$B_p = C_p + \bar{\imath} D_p. \tag{21}$$

Using eqns (13), (18), and (20) we obtain

$$IJ^{[k,i,j]} = (-1)^{i+j}(\cos(i+j)\theta_p J_p^{[k,i,j]} - \sin(i+j)\theta_p K_p^{[k,i,j]}) \tag{22a}$$

$$IK^{[k,i,j]} = (-1)^{i+j}(\sin(i+j)\theta_p J_p^{[k,i,j]} + \cos(i+j)\theta_p K_p^{[k,i,j]}) \tag{22b}$$

where

$$J_p^{[k,i,j]} = \tfrac{1}{2}(I_p^{[k,i,j]} + \bar{I}_p^{[k,i,j]}) \tag{23a}$$

$$K_p^{[k,i,j]} = \frac{1}{2\bar{\imath}}(I_p^{[k,i,j]} - \bar{I}_p^{[k,i,j]}) \tag{23b}$$

$$I_p^{[k,i,j]} = \int_{T_p}^{T_{p+1}} t_p^k \frac{(t_p - B_p)^p}{(t_p - \bar{B}_p)^q}\,\mathrm{d}t_p. \tag{24}$$

$\bar{I}$ and $\bar{B}$ are the complex conjugates of I and B of eqns (24) and (21) respectively.

The integrals $J_p^{[k,i,j]}$, $K_p^{[k,i,j]}$, $IL_p^{[k,i,j]}$ and $IP_p^{[k,i,j]}$ can be evaluated by the general recursive algorithm given in Vable (1985). It must be emphasized that the entire computation is carried out in the real plane and no complex arithmetic is used. The final results are analytical values of the integrals in eqns (17), (18) and (19). These recursive relations can also be used for determining continuity requirements and singularity contributions, as shown in Sections 5 and 6 respectively.

4.2. *Area integrals*

For the purposes of presentation we define

$$A_{ijk} = \int\int_R G_{ijk}(Q, P)p(P)\,\mathrm{d}x(P)\,\mathrm{d}y(P). \tag{25}$$

The area integrals are reduced to algebraic expressions by making two assumptions.

Assumption 1. We assume that the distributed load $p(P)$ is piecewise constant over N subregions R_n. The slopes, moments and shear forces all contain derivatives of the fundamental solution. By using Green's theorem we have

$$A_{ijk} = \sum_{n=1}^{N} -p(R_n) \oint G_{ij}(Q, P)n_k(P)\,\mathrm{d}s. \tag{26}$$

The minus sign is due to the fact that the integration is with respect to P while the derivatives are with respect to point Q. The transformation of the area integral in the displacement expression is achieved by noting that:

$$r^2 \ln(r) = \tfrac{1}{16}(r^4 \ln(r) - r^4/2)_{,ii}. \tag{27}$$

Using Green's formula it can be shown

$$A = -\frac{1}{4}\sum_{n=1}^{N} p(R_n) \oint_{B_n} (r_i n_i)(LG^{[2,0]} + LG^{[0,2]} - 0.25(PG^{[2,0]} + PG^{[0,2]}))\,ds. \tag{28}$$

It should be noted that the boundary B_n enclosing the domain element R_n can be of arbitrary shape. This is useful when the parts of the boundary B_n are the same as the actual boundary. In the interior the simplest approximation is a triangle. In this paper the entire region R_n is considered enclosed by a boundary made up from three parts. Each part can have any arbitrary shape.

Assumption 2. Assume each of the three parts can be represented by M_m straight line segments. Equation (26) can thus be represented as

$$A_{ijk} = -\sum_{n=1}^{N} p(R_n) \sum_{m=1}^{3} \sum_{p=1}^{M_m} n_k(P_p) \int_{B_p} G_{,ijk}(Q, P)\,ds(P). \tag{29}$$

With the last assumption we once more have integrals over straight lines. The term $r_i n_i$ in eqn (28) is the perpendicular distance from the field point Q to the pth line segment and equals D_p of eqn (21). Hence, all A values are linear combinations of the functions given by eqns (12)–(14). Thus the integrals in the equation are linear combinations of the integrals in eqns (17)–(19) with $k = 0$ and can be found in exactly the same manner as described in the previous section. It should be emphasized that recognition of the structure of the fundamental solution as given by the definition of the four functions in eqns (12)–(14) results in a simple algorithm that can be used for the analytical evaluation of the line and area integrals.

5. CONTINUITY REQUIREMENTS

The fundamental solutions in Table 1 are singular when the field point Q overlaps the source point P. The continuity requirements are established by answering the question: what are the conditions the unknown fictitious shear force V^* and the unknown fictitious moment M_n^* must satisfy in order for the integrals to remain bounded? The integrals containing the weak singular functions G, $G_{,i}$ and $G_{,ij}$ are always bounded. The singular functions $G_{,ijk}$ and $G_{,ijkm}$ contain first and second order singularities and yield the information we seek. These quantities appear in the expressions of $w_{,ij}$ and $w_{,ijk}$.

We will only consider the continuity requirements at a regular point on the boundary and not a corner. There is no loss of generality by letting the point Q approach the boundary from the interior along the normal direction (as shown in Fig. 4), as the continuity conditions

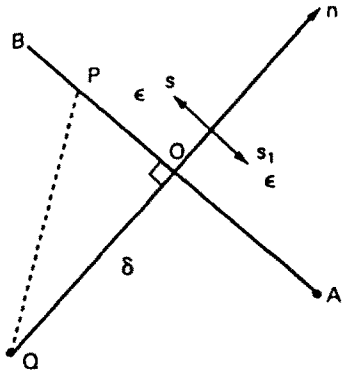

Fig. 4. Element geometry for establishing continuity requirements.

are not dependent on the path of Q. Let O be the point where Q touches the boundary. We draw two segments of length ε about point O. Let $S_{,ij}$ and $S_{,ijk}$ be the integrals in the expressions of $w_{,ij}$ and $w_{,ijk}$ in the vicinity of point O that may become unbounded. Thus

$$S_{,ij}(Q) = \int_{-\varepsilon}^{\varepsilon} G_{,ijm}(Q, P) n_m(P) M_n^*(P)\, \mathrm{d}s \tag{30a}$$

$$S_{,ijk}(Q) = \int_{-\varepsilon}^{\varepsilon} G_{,ijk}(Q, P) V^*(P)\, \mathrm{d}s + \int_{-\varepsilon}^{\varepsilon} G_{,ijkm}(Q, P) n_m(P) M_n^*(P)\, \mathrm{d}s. \tag{30b}$$

Expanding M_n^* about point O and using the integral formulas of Section 4 it can be shown that:

$$S_{xx} = -2\sin 2\theta (M_n^*(0^+) - M_n^*(0^-))(\ln(\varepsilon) - \ln(\delta)) - 2(1 - \cos 2\theta)(M_n^*(0^+) + M_n^*(0^-))\pi + \text{terms of order } \varepsilon \text{ and } \delta \tag{31}$$

where the superscripts + and − refer to the value of M_n^* just after and before point O. Similar expressions can be derived for other $S_{,ij}$. As Q approaches point O, that is $\delta \to 0$, one way of enforcing that S_{xx} remains bounded is to demand

$$M_n^*(0^+) = M_n^*(0^-). \tag{32}$$

The continuity of M_n^* is more restrictive than warranted by eqn (31). For if $|M_n^*(0^+) - M_n^*(0^-)| \leqslant K\delta$, then S_{xx} will remain bounded as $\delta \ln(\delta) \to 0$ as $\delta \to 0$. K refers to a positive number. The less restrictive condition is referred to as Holder's condition. However, it is not clear how one would enforce Holder's condition in BEM.

It should be emphasized that if $S_{,ij}$ is bounded then $w_{,ij}$ is bounded. This implies that moments M_{ij} and hence stresses must remain bounded. In problems such as rectangular holes in infinite plates, stresses at the corner are not bounded. Analysis of such problems must therefore permit discontinuities in M_n^* at the corners. Another point to note is that $w_{,ij}$ can be bounded and yet be discontinuous. Thus if finite discontinuity in stresses is being modeled then the continuity of M_n^* must be enforced.

The continuity of $w_{,ijk}$ is necessary if $w_{,ij}$ must be bounded. Hence the continuity of M_n^* is assumed in writing the following expression for S_{xxx}:

$$\begin{aligned} S_{xxx} = {} & (\cos 3\theta - 3\cos\theta)(V^*(0^+) - V^*(0^-))(\ln(\varepsilon) - \ln(\delta)) + (\sin 3\theta - 3\sin\theta) \\ & \times (V^*(0^+) + V^*(0^-))\pi - 6(\sin\theta - \sin 3\theta) M_n^*(0)/\varepsilon - 3(\sin 3\theta - \sin\theta) \\ & \times \left(\frac{\mathrm{d}M_n^*}{\mathrm{d}s}(0^+) - \frac{\mathrm{d}M_n^*}{\mathrm{d}s}(0^-)\right)(\ln(\varepsilon) - \ln(\delta)) + 3(\cos 3\theta - \cos\theta) \\ & \times \left(\frac{\mathrm{d}M_n^*}{\mathrm{d}s}(0^+) + \frac{\mathrm{d}M_n^*}{\mathrm{d}s}(0^-)\right)\pi. \end{aligned} \tag{33}$$

A simple way of enforcing that S_{xxx} remains bounded as $\delta \to 0$ is to demand that

$$V^*(0^+) = V^*(0^-) \tag{34}$$

$$\frac{\mathrm{d}M_n^*}{\mathrm{d}s}(0^+) = \frac{\mathrm{d}M_n^*}{\mathrm{d}s}(0^-). \tag{35}$$

The continuity of the fictitious shear force V^* and continuity of the slope of the fictitious moment M_n^* is more restrictive than necessary. The conditions

$$|V^*(0^+) - V^*(0^-)| \leqslant K_1\delta \quad \text{and} \quad \left|\frac{dM_n^*}{ds}(0^+) - \frac{dM_n^*}{ds}(0^-)\right| \leqslant K_2\delta,$$

referred to as Holder and Hadamard conditions, are less restrictive but it is not clear how one enforces these conditions in BEM. Once more it is emphasized that the continuity requirements of an equation do not preclude discontinuities in shear forces. The conditions only enforce that the discontinuities in the shear force remain finite.

5.1. *Choice of polynomial approximation*

The Lagrange polynomials ensure continuity of a function at element nodes as the coefficients of the polynomial are determined in terms of the nodal values of the function and are good choice for the approximation of the fictitious shear force V^*. The Hermite cubic polynomials ensure continuity of the function and its first derivatives as the coefficients of the polynomials are evaluated in terms of the nodal values of the function and its derivatives. The optimum choice of approximation would yield three unknowns per node (nodal values of fictitious shear force, nodal values of moment and its derivative). However, we need to satisfy two boundary conditions per collation point. This dichotomy leads to a cumbersome coding process. In this work the fictitious shear force and moment are approximated by the same polynomial, which will either be a Lagrange linear polynomial or a Hermite cubic polynomial. It should be emphasized that the cubic Lagrange polynomial approximation used by Vitooraporn and Moshaiov (1989) does not satisfy continuity of slopes at the element nodes. Thus the use of the cubic Lagrange polynomial may lead to poor results near the nodes on the boundary as slope continuity is not satisfied at these points.

6. SINGULARITY CONTRIBUTION

In this work no explicit expression for the singularity contribution is coded in the computer program. The iterative formulae of Vable (1985) are used when the field point Q is within a boundary element. To ensure correct computation, point Q is always chosen as the mid-point of a 2ε segment ($Q = O$ in Fig. 3). The limitation of this idea is that it cannot be used at corners. The analytical values of singularity contributions at a regular point as computed in the code are given below to elaborate a potential problem. The singularity contribution for the bending moment (SM_n) and the equivalent shear force (SV) were calculated from S_{ij} and S_{ijk} by enforcing the continuity conditions of eqns (32), (34) and (35). The values of the singularity contributions are:

$$SM_n = M_n^*/2. \tag{36}$$

$$SV = \frac{V^*}{2} + \left[\frac{(1-\nu)}{2R} + \frac{1+\nu}{2\varepsilon\pi}\right]M_n^*. \tag{37}$$

Note the coefficient of M_n^* in the expression for equivalent shear for SV. It contains the term of $1/\varepsilon$, which would seem to imply that as $\varepsilon \to 0$, equivalent shear force V will become unbounded. This does not happen as the term is independent of the element orientation and when the contributions from the other elements are added this term cancels out. This is the basic mechanism in the computation of the finite part of integrals containing higher order singularities. However, during computation a large number is added into the matrix and later subtracted. This addition and subtraction of large numbers can lead to a loss of significant figures. Therefore it may be worthwhile considering a regularization process for higher order singularities for analytical integration along the lines proposed by Rudolphi (1991) for numerical integration.

7. DIMENSIONLESS VARIABLES

Let L and M_0 be some characteristic length and moment. The dimensionless variables shown below with a hat are

$$\begin{aligned}
\hat{x}_i &= x_i/L \\
\hat{w} &= Dw/(M_0L^2) \\
\hat{w}_{,i} &= Dw_{,i}/(M_0L) \\
\hat{w}_{,ij} &= Dw_{,ij}/M_0 \\
\hat{w}_{,ijk} &= (DL)w_{,ijk}/M_0 \\
\hat{Q}_i &= Q_iL/M_0 \\
\hat{V}_i &= V_iL/M_0 \\
\hat{p} &= pL^2/M_0 \\
\hat{M}_n^* &= M_n^*/M_0 \\
\hat{V}^* &= V^*L/M_0.
\end{aligned} \tag{38}$$

Substituting the above definition into the integral equations (10), we obtain

$$\begin{aligned}
\hat{w}(Q) = &\oint_B \hat{G}(Q,P)\hat{V}^*(P)\,\mathrm{d}\hat{s} + \oint_B \hat{G}_{,i}(Q,P)n_i(P)\hat{M}_n^*(P)\,\mathrm{d}\hat{s} \\
&+ \int\int \hat{G}(Q,P)\hat{p}(P)\,\mathrm{d}\hat{x}(P)\,\mathrm{d}\hat{y}(P) + \ln(L)\left[\oint (\hat{r}^2\hat{V}^*(P) - 2\hat{r}_i n_i \hat{M}_n^*(P))\,\mathrm{d}\hat{s}\right].
\end{aligned} \tag{39}$$

If the last term in the square bracket is not zero, then the choice of the non-dimensionalizing parameter L will affect the displacement. Since the term in the square brackets is a quadratic in the field point coordinates the slope and the moments can also be affected by the choice of the parameter L. It can be confirmed that the following four conditions must be satisfied if the computed solution is to be independent of the parameter L:

$$R_i = \oint \left[f_i(P)V^*(P) - \frac{\partial f_i(P)}{\partial n(P)} M_n^*(P) \right] \mathrm{d}s = 0 \quad i = 1, \ldots, 4, \tag{40}$$

where $f_1 = 1$; $f_2 = x$; $f_3 = y$; $f_4 = (x^2 + y^2)$.

The first condition (R_1) implies that force equilibrium in the z-direction must be met by the fictitious shear force distribution. The second (R_2) and third (R_3) conditions imply that the moment equilibrium in the y- and x-directions respectively must be satisfied by the unknown distribution. The last condition (R_4) can be interpreted as a second moment of some kind. The conditions of eqn (40) are not explicitly enforced and may not be satisfied by the computed solution, as the numerical results demonstrate. Wu and Altiero (1981) reported that the choice of reference radius (the same as the parameter L) affected their results. There are two likely reasons for this. (i) Their unknown distribution did not satisfy the conditions of eqn (40). (ii) The conditioning of the matrix in the algebraic system may have been significantly affected, as discussed by Heise (1987). Work is in progress to overcome both these problems, as was done for elastostatics in Vable (1990). In this work the conditioning of the matrix and the value of the resultants R_i in eqn (40) will be monitored.

8. NUMERICAL RESULTS

Extensive numerical testing was conducted for all types of boundary conditions. Boundary data $(\bar{w}, \bar{\theta}, \bar{M}_n, \bar{V})$ were generated from a known analytical solution. Three kinds of boundary conditions were simulated and the computed solution was compared with the analytical solution at a number of points. The three types of boundary conditions that were simulated were the following.

Type 1: displacement and slopes were specified to simulate the clamped type boundary conditions.
Type 2: displacement and moments were specified to simulate simply supported boundary conditions.
Type 3: equivalent shear force and moments were specified to simulate the free edge boundary conditions.

Each problem was solved using linear Lagrange polynomials and then using cubic Hermite polynomials for the approximation of the unknowns, and the results are compared. In all problems the condition number of the matrix in the algebraic equation was computed. The matrix condition number was computed using the following definition:

$$\text{Matrix condition number} = \|A\| * \|A^{-1}\| \tag{41}$$

where $\|A\|$ and $\|A^{-1}\|$ are the norm of the matrix and its inverse respectively. The following definition for the norm of the matrix is used:

$$\|A\| = \max_i \sum_{j=1} |A_{ij}|.$$

The authors feel that the condition number of the matrix should be monitored for all algorithms as it reflects the sensitivity of the output data to small errors or changes in the input data, as shown in Vable (1987, 1990). The four parameters R_1–R_4 defined by equations were computed and are reported for each problem for reasons discussed in Section 7.

8.1. *Example* 1

The dimensionless displacement solution for a clamped circular plate under a uniform transverse load is given in Timoshenko and Woinowsky-Krieger (1959):

$$\hat{w} = (1-\hat{r}^2)^2/64 \tag{42}$$

where the non-dimensionalizing parameters L = radius of the plate and $M_0 = pL^2$. The plate boundary was uniformly divided into 24 elements [$M = 24$ in eqn (15)] for linear Lagrange approximation. Each of the elements was subdivided into four straight line [$N_m = 4$ in eqn (15)] segments. Boundary conditions were satisfied every 15°. Thus the total number of unknowns was 48. For the Hermite cubic approximation the boundary conditions were collocated at the same points. The boundary was made up of 12 elements ($M = 12$) with eight subdivisions. In other words the length of the cubic element was formed by combining two linear elements.

The area integral was evaluated using a single element [$N = 1$ in eqn (29)], as the transverse load is constant over the entire plate. The same nodes and elements as used for the line integrals were then used for evaluating the area integral.

Analytical values were compared with the computed values for the dimensionless displacement $\hat{w}$, moment $\hat{M}_x$ and shear force $\hat{Q}_x$. No appreciable difference was found between the linear and the cubic approximations and hence only results from the cubic

Table 2. Percentage errors in example 1

Coordinates		Boundary condition type 1			Boundary condition type 2			Boundary condition type 3		
r	θ	w	M_r	Q_r	w	M_r	Q_r	w	M_r	Q_r
0.00	0	0.06	0.03	—	2.24	1.12	—	211	0.02	—
0.50	0	0.08	0.09	0.00	2.99	3.07	0.00	374	0.02	0.00
0.90	0	0.29	0.02	0.01	11.75	1.06	0.01	*	0.03	0.01
0.95	0	0.47	0.01	0.04	22.84	0.84	0.04	*	0.01	0.03
0.99	0	0.94	0.39	0.55	220.0	0.34	0.55	*	0.02	0.41
1.00	0	—	0.72	1.00	—	0.00	1.00	—	0.00	0.75
1.00	15	—	0.65	1.00	—	0.10	1.00	—	0.00	0.75
1.00	30	—	0.45	1.01	—	0.42	1.00	—	0.01	0.75
1.00	45	—	0.03	0.99	—	1.06	1.00	—	0.03	0.75
R_1			−3.14			−3.12			−2.31	
R_4			−1.57			−1.57			−2.39	

approximation are reported in Table 2. The same type of boundary condition was specified at all points.

The results of Table 2 show good correlations with analytical results for moments and shear forces. Good correlations are also obtained for displacements when type 1 boundary conditions are imposed. Type 2 and 3 boundary conditions, however, show large errors for the displacements. The asterisk in Table 2 implies error in excess of 10,000%. The reason for these large errors is the presence of rigid body modes in the solution. If displacement is not specified at any point, such as in type 3 boundary conditions, then the body is free to translate. Similarly, if slope is not specified at any point, such as in type 2 and 3 boundary conditions, then the plate is free to rotate in the rigid body sense. From the computed results, if the rigid body mode is calculated (the numerically computed boundary values for displacement and slope were not zero) and accounted for, then the error was of the order of the type 1 boundary condition. Clearly this is an unacceptable procedure for practical problems. Work is in progress to determine and eliminate the rigid body mode, as was described for elastostatic problems in Vable (1987, 1990). It is worth noting that R_1 and R_4 are not zero for any type of boundary condition. R_2 and R_3 are nearly zero and are not reported. It is certain that the non-zero values of R_1 and R_4 contribute towards the error, but to what degree is not clear at this stage. In Table 3 the condition numbers for the two approximations for different boundary conditions are reported. For all boundary conditions the cubic approximation shows an order of magnitude higher condition numbers. These higher condition numbers imply a greater sensitivity to small changes or errors in the input data for the cubic approximation. The reason linear and cubic approximations yield the same percentage error was found in the behavior of the unknown. The first derivatives along the boundary for fictitious shear force and moment were found to be zero for this problem. In other words the fictitious shear force and moment were constant along the boundary for this problem. Thus the cubic approximation did not improve the approximation of the unknown as one had hoped.

8.2. *Example* 2

The dimensionless displacement solution for a simply supported square plate under a uniform transverse load is given in Timoshenko and Woinowsky-Krieger (1959):

Table 3. Comparison of matrix condition numbers in example 1

	Boundary condition type 1 ($\times 10^1$)	Boundary condition type 2 ($\times 10^1$)	Boundary condition type 3 ($\times 10^1$)
Linear	8.6	12.0	0.46
Cubic	2320	2270	72.4

$$w = \sum_{m=1,3,5}^{\infty} A_m \cosh(m,\pi\hat{y}) + B_m(m\pi\hat{y}) \sinh(m\pi\hat{y}) + C_m \sin(m\pi(x-0.5)) \tag{43}$$

$$A_m = -\left(\frac{m\pi}{2}\tanh\frac{m\pi}{2} + 2\right)B_m$$

$$B_m = 2\Big/\left(\pi^5 m^5 \cosh\frac{m\pi}{2}\right)$$

$$C_m = 4/\pi^5 m^5$$

where the non-dimensionalizing parameter L = the side of the square and $M_0 = pL^2$. The origin of the coordinate system is at the center of the plate. The boundary data $\hat{\theta}$, $\hat{M}_n$ and $\hat{V}$ can be easily generated by repeated differentiation of eqn (43). $\hat{M}_{ij}$ and $\hat{Q}_i$ can be found similarly. A computer program was written in which the series was truncated at $m = 91$. Boundary data were generated to simulate various boundary conditions. At each point on the boundary the same kind of boundary condition was specified for types 1 and 2. The type 3 boundary condition was not specified at all points because it would have resulted in a rigid body mode, as in example 1. Type 3 was specified on $\hat{y} = 0.5$ and on the remaining three sides the type 2 boundary condition was specified. It should be emphasized that at each corner either the displacement or the corner force [eqn (8)] should be enforced. However, this was not done in the solution process for a variety of reasons. The chief reason being that the variety of tricks suggested in the literature for modeling the corners have either not proved satisfactory or have limited application.

The problems were solved using linear Lagrange and cubic Hermite approximations. The mesh discretization was the same except that the length of a cubic element was constructed by combining two linear elements. The total number of unknowns for both approximations was 96. The boundary element solution was compared with the series solution and the percentage difference is reported in Table 4 for the linear approximation and Table 5 for the cubic approximation. Results are reported along the diagonal and $x = 0$.

The cubic approximation yields better results for all types of boundary conditions. Its results are an order of magnitude better than the linear approximation when type 3 boundary conditions are imposed on the edge $\hat{y} = 0.5$. For both approximations the results deteriorate as one approaches the corner. However, the accuracy of the linear approximation deteriorates more rapidly than for the cubic approximation. Near the corner $\hat{x} = \hat{y} = 0.49$, both approximates yield nonsensical results. It should be noted, however, that all three quantities ($\hat{w}$, $\hat{M}_x$ and $\hat{Q}_x$) approach zero near the corner. Thus small differences result in very large percentage errors. As one moves from the center towards the edge along $\hat{x} = 0$, the error increases as expected. It should be noted once more that $\hat{w}$ and $\hat{M}_x$ tend to zero near

Table 4. Percentage errors in example 2 for linear Lagrange approximation

Coordinates		Boundary condition type 1			Boundary condition type 2			Boundary condition type 3 on $y = 0.5$, type 2 elsewhere		
x	y	w	M_x	Q_x	w_1	M_x	Q_x	w	M_x	Q_x
0.00	0.00	0.14	0.06	—	0.51	0.36	—	9.47	6.67	—
0.20	0.20	0.16	0.07	0.26	0.33	0.01	1.09	8.62	4.11	30.9
0.40	0.40	1.48	2.46	109.0	6.46	76.3	192	23.1	185	9.13
0.45	0.45	1.04	60.5	1715	34.1	504	885	107	1160	180
0.00	0.20	0.16	0.18	0.30	0.41	0.07	0.20	6.26	0.60	8.4
0.00	0.40	0.13	0.38	1.11	0.51	0.93	1.59	4.81	3.17	0.44
0.00	0.45	0.10	0.25	2.19	0.63	1.39	5.03	4.28	3.28	4.06
0.00	0.49	0.22	30.9	3.82	1.20	18.4	11.4	1.62	18.2	10.7
R_1			−0.97			−0.94			−0.92	
R_4			−0.19			−0.18			−0.17	

Table 5. Percentage errors in example 2 for cubic Hermite approximation

Coordinates		Boundary condition type 1			Boundary condition type 2			Boundary condition type 3 on $y = 0.5$, type 2 elsewhere		
x	y	w	M_x	Q_x	w	M_x	Q_x	w	M_x	Q_x
0.00	0.00	0.01	0.01	—	0.14	0.10	—	0.64	0.39	—
0.20	0.20	0.01	0.01	0.04	0.16	0.14	0.00	1.06	0.85	0.46
0.40	0.40	0.12	0.33	2.80	0.44	2.07	0.45	3.10	4.83	5.97
0.45	0.45	0.40	4.80	43.4	0.91	15.4	22.2	2.58	18.6	43.0
0.00	0.20	0.01	0.01	0.04	0.14	0.10	0.08	0.69	0.55	0.01
0.00	0.40	0.01	0.08	0.60	0.16	0.22	0.21	0.82	1.19	0.89
0.00	0.45	0.06	0.39	1.56	0.16	0.25	0.14	0.89	1.43	1.95
0.00	0.49	0.49	11.7	3.45	0.13	0.26	0.17	0.14	8.54	7.52
R_1			−1.1			−1.1			−1.1	
R_4			−0.23			−0.23			−0.23	

Table 6. Comparison of matrix condition numbers in example 2

Approximation	Boundary condition type 1 ($\times 10^6$)	Boundary condition type 2 ($\times 10^6$)	Boundary condition type 3 on $y = 0.5$, type 2 elsewhere ($\times 10^6$)
Linear	25	73	8320
Cubic	24	479	8570

the edge, but in spite of this the results at $\hat{x} = 0.49$ are not unreasonable for the cubic approximation.

Table 6 shows the matrix condition numbers for the linear and cubic approximations. Once more the cubic approximation results in a higher condition number for all types of boundary condition. However, the differences are not as dramatic as in example 1.

9. CONCLUSIONS

The definition of the four functions in eqns (12)–(14) simplifies the description of the fundamental solution. It also reveals the structure of the fundamental solution that can be exploited for the analytical evaluation of line and area integrals. For stresses and shear forces to remain bounded the fictitious shear force and fictitious bending moment must be continuous. The first derivative of the fictitious moment must also be continuous. When the continuity conditions are met then the accuracy of the computed solution is better, as demonstrated by example 2. The matrix condition number, however, becomes worse when Hermite approximations are used to meet the continuity requirements, making the solution more sensitive to changes and error in the input data. This higher condition number is most likely because two collocation points are put in each element for the cubic Hermite approximation as opposed to a single collocation point for the linear Lagrange approximation. When the fictitious shear force and fictitious bending moment distributions do not satisfy the conditions given in eqn (40), then in addition to a rigid body mode, errors in moments are also possible. Work is in progress to improve the matrix conditioning and determine and account for the rigid body mode.

REFERENCES

Abdel-Akher, A. and Hartley, G. A. (1989). Evaluation of boundary integrals for plate bending. *Int. J. Numer. Meth. Engng* **28**, 75–93.

Altiero, N. J. and Sikarskie, D. L. (1978). A boundary integral method applied to plate of arbitrary plan form. *Comput. Struct.* **9**, 163–168.

Bezine, G. (1978). Boundary integral formulation for plate flexure with arbitrary boundary conditions. *Mech. Res. Commun.* **5**(4), 197–206.

Hartmann, F. (1986). The direct boundary element method in plate bending. *Int. J. Numer. Meth. Engng* **23**, 173–191.

Heise, U. (1987). Dependence of the round-off error in the solution of boundary integral equations on a geometrical scale factor. *Comput. Meth. Appl. Mech. Engng* **62**, 115–126.

Jawson, M. A., Matti, M. and Symm, G. T. (1967). Numerical biharmonic analysis and some applications. *Int. J. Solids Structures* **3**, 309–332.

Kaya, A. C. and Erdogan, F. (1987). On the solution of integral equations with strongly singular kernels. *Q. Appl. Math.* **XLV**(1), 105–122.

Kutt, H. R. (1975). The numerical evaluation of principal value integrals by finite-post integration. *Numer. Math.* **24**, 205–210.

Paris, F. and Leon, S. (1987). Boundary element method applied to the analysis of thin plates. *Comput. Struct.* **25**(2), 225–233.

Rudolphi, T. J. (1991). The use of simple solutions in the regularization of hyper singular boundary integral equations. *Math. Comp. Model.* **15**, 269–278.

Stern, M. (1979). A general boundary integral formulation for the numerical solution of plate bending problems. *Int. J. Solids Structures* **15**, 769–782.

Timoshenko, S. and Woinowsky-Krieger, S. (1959). *Theory of Plates and Shells*. McGraw-Hill, New York.

Tottenham, H. (1979). The boundary element method for plates and shells. In *Development in Boundary Element Methods* (Edited by P. K. Banerjee and R. Butterfield), pp. 173–205. Applied Science Publishers, London.

Vable, M. (1985). An algorithm based on the boundary element method for problems in engineering mechanics. *Int. J. Numer. Meth. Engng* **24**.

Vable, M. (1987). Making the boundary element method less sensitive to changes or errors in the input data. *Int. J. Numer. Meth. Engng* **26**.

Vable, M. (1990). Importance and use of rigid body mode in boundary element method. *Int. J. Numer. Meth. Engng* **29**, 453–472.

Vitooraporn, C. and Moshaiov, A. (1989). Effectiveness study of higher order elements in the boundary integral method for thin elastic plate bending. *Boundary Element Techniques: Application in Engineering* (Edited by C. A. Brebbia and M. G. Zamani), pp. 111–127. CMP, Boston.

Wu, B. C. and Altiero, N. J. (1981). A new numerical method for the analysis of anisotropic thin plate bending problems. *Comput. Meth. Appl. Mech. Engng* **25**, 343–353.

Zhang, Y. (1989). An indirect boundary element method for isotropic and orthotropic plates. Ph.D. dissertation, Michigan Technological University.